HHS Public Access

Author manuscript

Neuropharmacology. Author manuscript; available in PMC 2021 October 15.

Published in final edited form as:

Neuropharmacology. 2020 October 15; 177: 108195. doi:10.1016/j.neuropharm.2020.108195.

Pharmacodynamics and pharmacokinetics of the novel synthetic opioid, U-47700, in male rats

Michael T. Truver[1], **Christina R. Smith**[1], **Nancy Garibay**[2], **Theresa A. Kopajtic**[3], **Madeleine J. Swortwood**[1,*], **Michael H. Baumann**[2,*]

[1]Department of Forensic Science, College of Criminal Justice, Sam Houston State University, Huntsville, TX, USA

[2]Designer Drug Research Unit, Intramural Research Program, National Institute on Drug Abuse, Nation Institute of Health, Baltimore, MD, USA

[3]Biobehavioral Imaging and Molecular Neuropsychopharmacology Unit, Intramural Research Program, NIDA, NIH, Baltimore, MD, USA

Abstract

Novel synthetic opioids are appearing in recreational drug markets worldwide as adulterants in heroin or ingredients in counterfeit analgesic medications. Trans-3,4-dichloro-*N*-[2-(dimethylamino)cyclohexyl]-*N*-methyl- benzamide (U-47700) is an example of a non-fentanyl synthetic opioid linked to overdose deaths. Here, we examined the pharmacodynamics and pharmacokinetics of U-47700 in rats. Male Sprague-Dawley rats were fitted with intravenous (i.v.) catheters and subcutaneous (s.c.) temperature transponders under ketamine/xylazine anesthesia. One week later, rats received s.c. injections of U-47700 HCl (0.3, 1.0 or 3.0 mg/kg) or saline, and blood samples (0.3 mL) were withdrawn via i.v. catheters at 15, 30, 60, 120, 240, 480 min post-injection. Pharmacodynamic effects were assessed at each blood withdrawal, and plasma was assayed for U-47700 and its metabolites by liquid chromatography tandem mass spectrometry. U-47700 induced dose-related increases in hot plate latency (ED_{50}=0.5 mg/kg) and catalepsy (ED_{50}=1.7 mg/kg), while the 3.0 mg/kg dose also caused hypothermia. Plasma levels of U-47700 rose linearly as dose increased, with maximal concentration (C_{max}) achieved by 15–38 min. C_{max} values for *N*-desmethyl-U-47700 and *N,N*-didesmethyl-U-47700 were delayed but reached levels in the same range as the parent compound. Pharmacodynamic effects were correlated with plasma

*Corresponding authors: Michael H. Baumann, Ph.D., Designer Drug Research Unit, IRP, NIDA, NIH, Baltimore, MD 21224, mbaumann@mail.nih.gov, Madeleine J. Swortwood, Ph.D., College of Criminal Justice, Sam Houston State University, Huntsville, TX 77340, swortwoodm@shsu.edu.

CREDIT AUTHOR STATEMENT

MTT: Methodology, Formal analysis, Investigation, Writing Original Draft

CRS: Methodology, Validation, Investigation

NG: Investigation, Formal analysis

TAK: Investigation, Formal analysis

MJS: Conceptualization, Resources, Data curation, Writing Review & Editing, Supervision

MHB: Conceptualization, Methodology, Formal analysis, Resources, Writing Review & Editing, Supervision, Project Administration, Funding Acquisition

U-47700 and its *N*-desmethyl metabolite. Using radioligand binding assays, U-47700 displayed high affinity for μ-opioid receptors (Ki=11.1 nM) whereas metabolites were more than 18-fold weaker. Our data reveal that U-47700 induces typical μ-opioid effects which are related to plasma concentrations of the parent compound. Given its high potency, U-47700 poses substantial risk to humans who are inadvertently exposed to the drug.

Keywords

analgesia; catalepsy; metabolites; opioid; U-47700

1. Introduction

Since 2013, illicitly-manufactured fentanyl has fueled an epidemic of overdose fatalities in the Unites States (U.S.) and elsewhere (1). To add to this crisis, an increasing number of novel synthetic opioids (NSOs) are appearing in recreational drug markets as heroin adulterants or ingredients in counterfeit analgesic medications (2). Trans-3,4-dichloro-*N*-[2-(dimethylamino)cyclohexyl]-*N*-methyl- benzamide (U-47700) is an example of a non-fentanyl NSO that was first encountered between 2015–2016 (3) (see Figure 1 for chemical structure). Originally developed as a candidate medication by the Upjohn Company in the 1970's, U-47700 and related analogs are now being diverted for recreational misuse. An early preclinical investigation demonstrated that U-47700 is a μ-opioid receptor agonist in mice, with analgesic potency 7.5-times greater than morphine (4). In a more recent study, we confirmed that U-47700 is a selective and efficacious μ-opioid receptor agonist that has greater potency than morphine (5). While pharmacological information from human subjects is limited, it is tempting to speculate that U-47700 is abused due to its euphoric and analgesic effects.

U-47700 is implicated in many overdose deaths, though most cases were polysubstance users who tested positive for other illicit drugs (2,3). The reported whole blood concentrations of U-47700 from fatal overdose victims ranged from 8–3040 ng/mL (6–19), whereas whole blood concentrations from non-fatal intoxications ranged from 94–351 ng/mL (20,21). Krotulski *et al* were the first to examine biotransformation of U-47700 using human liver microsomes and identified four main metabolites (22), with the principal compound being *N*-desmethyl-U-47700 (see Figure 1). Richeval *et al* analyzed human urine specimens from subjects exposed to U-47700 and found the same metabolites noted by Krotulski *et al* (12). Other investigations employed structure elucidation on authentic samples to predict U-47700 metabolites and have determined that *N*-desmethyl and *N,N*-didesmethyl compounds predominate (10,23). No study has examined the pharmacokinetics or biological activity of U-47700 metabolites.

From a forensic standpoint, only two analytical methods have been reported for the quantitation of U-47700 and its metabolites (24,25). Rojek *et al* developed and validated a method to detect U-47700 and its metabolites in blood, and applied the method to postmortem human samples (N=12). More recently, our laboratory developed and validated a sensitive method for the quantification of U-47700, *N*-desmethyl-U-47700, and *N,N*-

didesmethyl-U-47700 in human plasma utilizing liquid chromatography tandem mass spectrometry (LC-MS/MS), and cross validated the method in rat plasma (24). A major difference between the two reported analytical methods is that during optimization, we were able to chromatographically separate *N,N*-didesmethyl-U-47700 from a co-eluting peak observed in the Rojek study.

In order to better understand the pharmacology of U-47700, the pharmacokinetic profiles and bioactivity of drug metabolites should be evaluated. To date, no studies have examined pharmacodynamic and pharmacokinetic relationships for U-47700 in either humans or animal models. To this end, we employed our analytical method (24) to quantify U-47700 and its metabolites in plasma samples obtained from male rats treated with subcutaneous (s.c.) U-47700 (0.3, 1.0, and 3.0 mg/kg). Rats for our study were fitted with indwelling intravenous (i.v.) catheters for repeated blood sampling, and pharmacodynamic endpoints were assessed at each blood withdrawal. Thus, our experimental design allowed for assessment of pharmacodynamic and pharmacokinetic endpoints in the same subjects. In separate experiments, we employed radioligand binding methods in post-mortem rat brain tissue to examine opioid receptor affinities for U-47700 and its *N*-desmethyl metabolites.

2. Materials and Methods

2.1. Reagents and Chemicals

U-47700, U-47700 HCl, *N*-desmethyl-U-47700, *N,N*-didesmethyl-U-47700, and U-47700-d6 were purchased from Cayman Chemical Company (Ann Arbor, MI, USA). Chemicals and reagents used for extraction and LC-MS/MS were the highest purity available. Pooled blank male Sprague Dawley rat plasma preserved with sodium heparin was obtained from BioIVT (Medford, MA, USA). Sterile 0.9 % NaCl (saline) was obtained by Hospira, Inc (Lake Forest, IL, USA), while heparin saline (1000 IU/mL) was purchased from Thomas Scientific (Swedesboro, NJ, USA). U-47700 HCl was dissolved in saline for s.c. administration.

2.2 Animals and Surgery

Male Sprague-Dawley rats (300–400 g) purchased from Envigo (Frederick, MD, USA) were double-housed under conditions of controlled temperature (22±2°C) and humidity (45±5%), with *ad libitum* access to food and water. Lights were on from 7:00 AM to 7:00 PM. The National Institute on Drug Abuse (NIDA), Intramural Research Program (IRP), Animal Care and Use Committee approved the animal experiments, and all procedures were carried out in accordance with the NIH Guide for the Care and Use of Laboratory Animals. Vivarium facilities were fully accredited by the Association for Assessment and Accreditation of Laboratory Animal Care. Experiments were designed to minimize the number of animals included in the study.

Rats received a mixture of intraperitoneal (i.p.) ketamine (75 mg/kg) and xylazine (5 mg/kg) for surgical anesthesia. Once a rat was fully anesthetized, an i.v. catheter constructed of Silastic® (Dow Corning, Midland, MI, USA) and vinyl tubing was surgically implanted into the right jugular vein. Briefly, the proximal Silastic end of the catheter was advanced to the

atrium whereas the distal vinyl end was exteriorized on the nape of the neck and plugged with a metal stylet. Immediately after catheter implantation, while still under anesthesia, each rat received a s.c. temperature transponder (model IPTT-300, Bio Medic Data Systems, Seaford, DE, USA) to allow for the non-invasive measurement of body temperature (26). The temperature transponder emits radio frequency signals that are received by a compatible hand-held reader system (DAS-7006/7r, Bio Medic Data Systems). Transponders are cylindrical in shape, 14 × 2 mm, and were implanted on the back via a pre-packaged sterile guide needle. Rats were single-housed post-operatively and given at least 1 week to recover.

2.3. Experimental procedures

On the day of an experiment, rats were brought into the laboratory in their home cages and allowed 1 h to acclimate. Polyethylene extension tubes were attached to 1 mL tuberculin syringes, filled with sterile saline, and connected to the vinyl end of the catheters. The extension tubes were threaded outside the cages to facilitate blood sampling by an investigator remote from the animal. Catheters were flushed with 0.3 mL of 48 IU/mL heparin saline to facilitate blood withdrawal. Groups of rats (N=6 per group) received s.c. injections of either saline vehicle (control) or U-47700 (0.3, 1.0, and 3.0 mg/kg) on the lower back between the hips. We chose the s.c. route of administration to allow for the comparison of our pharmacodynamic findings in rats to those reported for mice that received s.c. U-47700 (4,5). Rats were randomly assigned to each dose group. Blood samples (300 μL) were withdrawn via catheters immediately before (t=0) and at 15, 30, 60, 120, 240, and 480 min following injection. Samples were collected into 1 mL tuberculin syringes, then transferred to 1.5 mL plastic tubes containing 5 μL of 250 mM sodium metabisulfite as a preservative and 5 μL of 1,000 IU/mL heparin as an anticoagulant. Blood was centrifuged at 1000 g for 10 min at 4°C. Plasma was decanted into cryovials and stored at −80°C until analysis. After each blood withdrawal, an equal volume of saline solution was infused via the i.v. catheter to maintain volume and osmotic homeostasis.

Pharmacodynamic endpoints including catalepsy score, body temperature, and hot plate latency, were determined at each blood withdrawal. Behavior was observed by an experienced rater blind to drug treatment for 1 min prior to blood withdrawal. During the 1 min observation period, catalepsy was scored based on three overt symptoms: immobility, flattened body posture, and splayed limbs. Each symptom was scored as either 1=absent or 2=present, and catalepsy scores at each time point were summed (yielding a minimum score of 3 and a maximum score of 6). Next, body temperature was rapidly measured using a handheld reader sensitive to signals emitted by the surgically-implanted transponder. We chose to examine hypothermia as a representative adverse effect of U-47700, since body temperature is easy to measure non-invasively and it decreases in parallel with opioid-induced bradycardia and respiratory depression (27). Blood samples were withdrawn immediately after temperature recording. After the blood draw, rats were placed on a hot plate analgesia meter (IITC Life Sciences, Woodland Hills, CA, USA) set at 52°C. Rats remained on the hot plate until they exhibited paw licking, flinching, or jumping in response to the heat stimulus, and were then returned to their home cages. Time spent on the hot plate was recorded using a timer triggered by a foot pedal. A 45 sec cut-off was employed to prevent tissue damage.

2.4. Quantification of U-47700 and its Metabolites in Plasma

Plasma was analyzed using our previously validated method (Smith *et al*) (24). Briefly, internal standard was added to plasma (100 μL) and buffered before loading onto solid phase extraction cartridges. Analytes were eluted with dichloromethane:isopropyl alcohol (80:20, v/v) with 5% ammonium hydroxide, then dried under nitrogen and reconstituted in 50 μL of 5 mM ammonium formate with 0.05% formic acid in water: 0.1% formic acid in methanol (60:40, v/v). Samples were analyzed on an Agilent 1290 Infinity II Liquid Chromatograph system equipped with an Agilent 6470 Triple Quadrupole Mass Spectrometer (Santa Clara, CA, USA). Agilent MassHunter Software was used for data acquisition and analysis of U-47700, *N*-desmethyl-U-47700, and *N,N*-didesmethyl-U-47700. Linear ranges were 0.1–100 ng/mL for U-47700 and *N*-desmethyl-U-47700, and 0.5–100 ng/mL for *N,N*-didesmethyl-U-47700. The limits of detection were 0.05 ng/mL for U-47700 and *N*-desmethyl-U-47700 and 0.1 ng/mL for *N,N*-didesmethyl-U-47700.

2.5. Radioligand binding

Opioid receptor binding assays were carried out as described previously (28). Whole rat brains minus cerebellum (BioIVT, Medford, MA, USA) were thawed on ice, homogenized in 50 mM Tris HCl at pH 7.5 using a Brinkman Polytron (setting 6 for 20 sec), and centrifuged at 30,000 g for 10 min a 4° C. The supernatant was discarded, and the pellet was resuspended in fresh buffer and spun again at 30,000 g for 10 min. The pellet was resuspended to yield 100 mg/mL wet weight. Ligand binding experiments were conducted in polypropylene tubes containing 500 μL Tris buffer and 100 μL of tissue suspension for 1 h at room temperature. Radioligands were used at 1 nM final concentration. Specifically, [^{3}H]DAMGO (Poly Peptide Laboratories, San Diego, CA, USA), [^{3}H]DADLE (Poly Peptide Laboratires, San Diego, CA, USA) and [^{3}H]U69,593 (Perkin Elmer Life Sciences, Waltham, MA, USA) were used to label μ-, δ-, and κ-opioid receptors, respectively. Non-specific binding was determined in the presence of 10 μM naloxone in all cases. Incubations were terminated by rapid vacuum filtration over Whatman GF/B filters using a cell harvester (Brandel Instruments, Gaithersburg, MD, USA). Filters were washed twice with ice cold buffer, transferred to scintillation vials, and Cytoscint (MP Biomedicals, Irvine, CA, USA) was added. Vials were counted the following day using a Perkin Elmer TriCarb liquid scintillation counter.

2.6. Data Analysis

All statistical analyses were carried out using Graph Pad Prism V.7 (San Diego, CA, USA) unless otherwise noted. Pharmacodynamic and pharmacokinetic data were analyzed by two-way (treatment × time) analysis of variance (ANOVA) followed by Tukey's *post hoc* tests. Plasma pharmacokinetic data were further evaluated using APL Pharmacokinetic Modeling Program (PKMP) to determine non-compartmental parameters such as half-life ($t_{1/2}$), area-under-the-curve (AUC), and maximal concentration (C_{max}). The possibility of non-linearity for plasma analyte concentrations was evaluated by calculating expected values for AUC and comparing with observed values. The 0.3 mg/kg observed AUC values for each analyte were multiplied by 3.3 and 10 in order to calculate the expected AUC values for the 1.0 and 3.0 mg/kg doses, respectively. The data from observed and expected AUC were compared using

nonparametric t-tests. Relationships between pharmacodynamic and pharmacokinetic endpoints were evaluated using Pearson correlation analyses, while hot plate latency data and plasma U-47700 concentrations were used to create hysteresis plots. Ki values for the radioligand binding data were determined using nonlinear regression analysis.

3. Results

3.1. Pharmacodynamic Effects of U-47700

The pharmacodynamic effects produced by U-47700 are shown in Figure 2. Rats that received s.c. saline injections displayed hot plate latencies that did not change post-injection, whereas those that received U-47700 showed dose-dependent ($F[3,20]=63.9$, $p<0.0001$) and time-dependent ($F[6,20]=106.8$, $p<0.0001$) increases in hot plate latency, indicative of an analgesic effect. *Post hoc* tests demonstrated that rats receiving the low dose of U-47700 (0.3 mg/kg) showed significant increases in hot plate latency only at 15 min, whereas the higher doses induced more sustained effects. Rats that received 1.0 and 3.0 mg/kg U-47700 exhibited the maximum cut-off latency of 45 seconds by 15–30 mins post-injection. Nonlinear regression of the mean hot plate responses over the first 120 min after injection revealed an ED_{50} of 0.5 mg/kg. Rats that received saline injection displayed no evidence of catalepsy, but rats that received U-47700 showed dose-dependent ($F[3,20]=26.2$, $p<0.0001$) and time-dependent ($F[6,20]=37.9$, $p<0.0001$) increases in immobility, flattened body posture, and splayed limbs, indicators of catalepsy. The lowest dose of U-47700 did not produce a significant change in catalepsy when compared to saline treatment, whereas the 1.0 and 3.0 mg/kg doses caused a rapid rise in catalepsy scores. Similar to the hot plate findings, rats exhibited the highest catalepsy scores at 15–30 min post-injection, with 3.0 mg/kg U-47700 producing maximal scores at the 30 min time point. Nonlinear regression of the mean catalepsy scores during the first 120 min after injection revealed an ED_{50} of 1.7 mg/kg. U-47700 produced dose-dependent ($F[3,20]=11.5$, $p<0.0001$) and time-dependent ($F[6,20]=20.6$, $p<0.0001$) changes in core body temperature. *Post hoc* tests demonstrated that only the 3.0 mg/kg dose of U-47700 significantly altered temperature, with a robust hypothermic response from 30–120 min post-injection.

3.2. Pharmacokinetics of U-47700 and its Metabolites

Time-concentration profiles for plasma U-47700, *N*-desmethyl-U-47700, and *N,N*-didesmethyl-U-47700 are shown in Figure 3. Pharmacokinetic data represent free, unconjugated analytes, as hydrolysis was not performed. Data depicted in Figure 3 were obtained from the same subjects shown in Figure 2, and findings from the time-concentration profiles were used to derive pharmacokinetic constants presented in Table 1. U-47700 plasma concentrations increased in a dose-dependent ($F[2,14]=107.2$, $p<0.0001$) and time-dependent ($F[6,14]=142.9$, $p<0.0001$) manner. C_{max} values were 40, 110, and 173 ng/mL for the 0.3, 1.0, and 3.0 mg/kg doses, and the corresponding AUC values were 2169, 9872, and 26,692 min*ng/mL, respectively. T_{max} for U-47700 was achieved rapidly within 15–38 min, while $t_{1/2}$ values ranged from 68–102 min. *N*-desmethyl-U-47700 plasma concentrations rose in a dose-dependent ($F[2,14]=17.0$, $p<0.0001$) and time-dependent ($F[6,14]=14.0$, $p<0.0001$) manner. *N*-desmethyl-U-47700 C_{max} values were less than those of U-47700 at all doses, and T_{max} was delayed when compared to the parent compound. AUC

values for *N*-desmethyl-U-47700 were 1289, 8158, and 33,881 min*ng/mL for 0.3, 1.0, and 3.0 mg/kg doses of U-47700, respectively. The plasma $t_{1/2}$ values for *N*-desmethyl-U-47700 were 110 and 136 min after administration of the 0.3 and 1.0 doses of U-47700. After the 3.0 mg/kg dose of U-47700, there were insufficient data points on the descending limb of the *N*-desmethyl time-concentration curve to calculate $t_{1/2}$. The plasma concentrations of *N,N*-didesmethyl-U-47700 increased in a dose-dependent ($F[2,14]=9.7$, $p<0.001$) and time-dependent manner ($F[6,14]=37.9$, $p<0.0001$), though this metabolite had even slower kinetics. C_{max} values for *N,N*-didesmethyl-U-47700 were comparable to that of U-47700. The $t_{1/2}$ values for *N,N*-didesmethyl-U-47700 were 126 and 301 min for 0.3 and 1.0 mg/kg U-47700. The $t_{1/2}$ for *N,N*-didesmethyl-U-47700 could not be determined for the 3.0 mg/kg dose of U-47700, since the metabolite concentrations were still rising at 480 min post-injection. *N,N*-didesmethyl-U-47700 displayed the largest AUC among all analytes, with values of 6427, 34,463, and 69,834 min*ng/mL for 0.3, 1.0 and 3.0 mg/kg U-47700 doses.

By comparing expected AUC values to the observed AUC values, the possibility of non-linear accumulation of U-47700 and its metabolites was evaluated. These findings are summarized in Figure 4 for U-47700, *N*-desmethyl-U-47700, and *N,N*-didesmethyl-U-47700. The only analyte with an observed AUC value greater than its expected AUC value was *N*-desmethyl-U-47700, though this difference was only statistically significant for the 3.0 mg/kg U-47700 dose ($T[9]=2.433$, $p<0.05$).

3.3. Correlative Relationships

Pharmacodynamic and pharmacokinetic data were obtained from the same subjects in our study which enabled the use of Pearson correlation analyses to evaluate relationships among various endpoints. Plasma U-47700 concentrations were significantly correlated with hot plate latency ($r=0.8547$, $p<0.001$), catalepsy scores ($r=0.8512$, $p<0.001$), and core body temperature ($r=-0.2918$, $p<0.001$). Likewise, *N*-desmethyl-U-47700 concentrations were correlated with hot plate latency ($r=0.3420$, $p<0.0001$), catalepsy ($r=0.2537$, $p<0.01$) and temperature ($r=-0.5997$, $p<0.001$). By contrast, *N,N*-didesmethyl-U-47700 was marginally correlated only with temperature ($r=-0.2163$, $p<0.02$). Because analgesia is a defining feature of opioid agonists, we created hysteresis plots using mean hot plate latency data and corresponding plasma U-47700 concentrations at each dose. Hysteresis plots are shown in Figure 5. At the 1.0 and 3.0 mg/kg doses of U-47700, the hysteresis progression was determined to be counter clockwise. The highest plasma concentrations of U-47700 at these doses were achieved at 30 min, and this corresponded to the maximal hot plate latency.

3.4. Radioligand Binding Results

Since metabolites of U-47700 were found at high concentrations in the bloodstream, and levels of *N*-desmethyl-U-47700 were correlated with all pharmacodynamic endpoints, we examined opioid receptor binding affinities for the parent compound and its metabolites. Morphine was included as a standard comparator drug. Opioid receptor binding data are summarized in Table 2. As expected, U-47700 had high affinity for μ-opioid receptors ($K_i=11.1$ nM) when compared to its affinity for δ-opioid ($K_i=1220$ nM) and κ-opioid receptors ($K_i=287$ nM), with μ/δ and μ/κ ratios of 110 and 26, respectively. U-47700 displayed slightly less affinity for μ-opioid receptors when compared to morphine ($K_i=2.7$

nM), but the two compounds had similar receptor selectivity. *N*-desmethyl-U-47700 displayed an 18-fold lower μ-opioid receptor affinity (Ki=206 nM) when compared to the parent compound, and was less selective. *N*,*N*-didesmethyl-U-47700 was even weaker at μ-opioid receptors (Ki=4,080 nM) and had a non-selective receptor binding profile.

4. Discussion

The aim of the present investigation was to characterize the pharmacodynamic and pharmacokinetic relationships for U-47700, a non-fentanyl NSO that has been implicated in numerous overdose fatalities in the US and elsewhere (6–19). U-47700 was initially developed as an analgesic medication in the 1970s, but the compound was never approved for clinical use and is now being diverted in recreational drug markets worldwide (2,3). Despite its widespread availability and misuse, little information is available about the pharmacology of U-47700 (4,5), especially with regard to *in vivo* pharmacokinetics and metabolism. We found that U-47700 produces typical opioid-mediated analgesia and catalepsy in rats, with *in vivo* potency estimates that are greater than those reported for morphine (29,30). Plasma concentrations of U-47700 rose rapidly, achieved C_{max} values within 15–38 min, and declined steadily thereafter. By contrast, plasma concentrations of *N*-desmethyl metabolites increased at a slower rate and persisted in the bloodstream. *N*,*N*-didesmethyl-U-47700 displayed especially slow elimination, suggesting this metabolite might serve as a sustained marker for U-47700 exposure in humans. Pharmacodynamic effects were significantly correlated with plasma U-47700 and *N*-desmethyl-U47700 but less so with *N*,*N*-didesmethyl-U47700. Importantly, U-47700 had high affinity for μ-opioid receptors (Ki=11.1 nM) while metabolites were much weaker in this respect, indicating that metabolites probably do not contribute to the pharmacodynamic effects of the parent drug *in vivo*.

As far as we are aware, the present findings represent the only information about pharmacodynamic effects of U-47700 in rats. Cheney *et al* demonstrated that U-47700 is a μ-opioid agonist in CF-1 mice with an ED_{50}=0.2 mg/kg in the tail flick assay (4) and our recent data confirm this observation in CD-1 mice (5). Here we demonstrate that U-47700 has an ED_{50}=0.5 mg/kg s.c. in the rat hot plate assay, and this potency value is identical to our previous findings for the tail flick test in C57Bl/6J mice. Although we did not test morphine in the present experiments, reported ED_{50}s for morphine in the rat hot plate test range from 5.0–9.0 mg/kg (29,31), indicating that U-47700 is approximately 10-fold more potent than morphine as an analgesic agent in rats. U-47700 also produced dose-dependent catalepsy that was characterized by immobility, flattened body posture, and splayed limbs. The ED_{50} for U-47700 to induce catalepsy was right-shifted (i.e., ED_{50}=1.7 mg/g) when compared to effects of the drug in the hot plate test, and this observation agrees with the findings of others who found that higher doses of morphine are required to produce catalepsy when compare to analgesia (30,32). U-47700 produced marked hypothermia at the highest dose tested (3.0 mg/kg), and we recently reported similar decreases in rat body temperature after administration of the ultrapotent fentanyl analog, carfentanil (33). It is well established that effects of μ-opioid agonists on body temperature are biphasic, with hyperthermia at low doses but hypothermia at higher doses (34). We found no evidence for hyperthermia after U-47700, but the dose required to significantly reduce body temperature

was much greater than the doses producing analgesia. Geller *et al* noted hypothermic responses in rats given s.c. morphine doses greater than 32.0 mg/kg (34), again suggesting that U-47700 is about 10-fold more potent than morphine in the rat. While we used hypothermia as endpoint for adverse effects of U-47700, it is important to note that hypothermia and respiratory depression may not always correlate. These two phenomena could be mediated by different intracellular signaling pathways and be influenced by biased agonism, for example. Wong et al., 2017, have shown a correlation between hypothermia and respiratory depression in an inhaled carfentanil model (27), but not using other opioids. Thus, further research is warranted to examine the dose-response for U-47700 to induce respiratory depression in rodent models.

No previous studies have examined the pharmacokinetics of U-47700 in animal models. Here we show that U-47700 achieves plasma C_{max} within 15–38 min of s.c. administration and displays a $t_{1/2}$=68–102 min, indicating rapid absorption, metabolism and elimination in rats. By comparison, the $t_{1/2}$ for morphine in the rat is reported to be 40–115 min, regardless of route of administration (35,36). Concentrations of U-47700 in blood and serum obtained from non-fatal human intoxications range from 8–251 ng/mL in blood and serum (20,21,23,37,38). Of these concentrations, Jones *et al* were the only investigators to report a concentration of U-47700 (228 ng/mL in serum) without the presence of any other illicit drugs of abuse (23). Extrapolation of data from rats to humans must be made with caution, yet the C_{max} values for U-47700 that we observed in rats (40–173 ng/mL) are comparable to the blood concentrations observed in forensic casework. Such findings suggest that our rat model has translational value, at least in terms of absolute concentrations of parent drug in the bloodstream. On the other hand, Koch *et al* determined the $t_{1/2}$ of U-47700 to be 6 h in humans, based on data from a patient who eventually died from overdose (16). The human $t_{1/2}$ value was calculated by taking several blood samples during hospitalization and plotting the concentration-time curve. It seems obvious that the present study in rats is not directly comparable to a human patient intoxicated with U-47700. Nevertheless, the disparity between the $t_{1/2}$ measured in rats versus that reported by Koch *et al* may reflect a fundamental difference between rats and humans, whereby the former display much faster clearance of most xenobiotics when compared to the latter (39,40).

The current findings characterized the *in vivo* pharmacokinetics of U-47700 metabolites for the first time in any species. The *N*-desmethyl metabolites of U-47700 were identified by Krotulski *et al* using human liver microsomes *in vitro* (22), and the present data confirm that rats form the same metabolites *in vivo*. Importantly, *N*-desmethyl-U-47700 and *N,N*-didesmethyl-U-47700 are found at concentrations in the same range as the parent compound, and they display longer $t_{1/2}$ values. *N,N*-didesmethyl-U-47700 had an especially slow elimination time, with concentrations still rising 480 min after the 3.0 mg/kg dose of U-47700. The elevations in *N,N*-didesmethyl-U-47700 increased linearly as the dose of U-47700 increased, whereas the concentrations of *N*-desmethyl-U-47700 appeared to accumulate in a nonlinear fashion. While we have no ready explanation for these observations, it seems possible that metabolic conversion of *N*-desmethyl-U-47700 to its *N,N*-didesmethyl product is saturable or perhaps rate limiting. In any case, our findings with U-47700 metabolites support the work of Richeval *et al* who suggested that *N*-desmethyl

metabolites of U-47700 could be used as forensic indicators of drug exposure that significantly increase the time frame for detection (12).

Because we examined pharmacodynamic effects and pharmacokinetic measures in the same subjects, we were able to examine correlative relationships among the various endpoints. We found that hot plate latency, catalepsy scores, and hypothermia were all significantly correlated with circulating concentrations of U-47700 and *N*-desmethyl-U-47700. These findings imply that *N*-desmethyl-U-47700 might be involved in mediating pharmacodynamic effects of systemically-administered U-47700. However, the radioligand binding data clearly show that *N*-desmethyl-U47700 displays much weaker affinity for μ-opioid receptors (Ki=206 nM) when compared to the parent compound U-47700 (Ki=11.1 nM). The *N,N*-didesmethyl metabolite is even less potent and essentially inactive at μ-opioid receptors (Ki=4,080 nM). The binding data reveal important structure-activity information showing sequential removal of *N*-methyl groups from the cyclohexyl amine of U-47700 produces corresponding decreases in μ-opioid receptor affinity. Perhaps most importantly, the radioligand binding data indicate that metabolites of U-47700 probably do not contribute to pharmacodynamic effects of systemically-administered U-47700. Pain relief is a defining feature of μ-opioid receptor agonists. Here we show that plasma concentrations of U-47700 are positively and significantly correlated with hot plate latency, and this relationship displays counterclockwise hysteresis. Other investigators have shown a similar counterclockwise hysteresis when examining the relationship between morphine and analgesic effects in rats. Van Crugten *et al* have attributed the lag between plasma morphine concentrations and observed pharmacological effects to the time required for the drug to cross the blood-brain barrier (41). The counter clockwise hysteresis observed in the current study could also be related to blood-brain barrier penetration of U-47700.

To conclude, we provide the first pharmacological characterization of the non-fentanyl synthetic opioid U-47700 in rats. U-47700 displays high affinity for the μ-opioid receptor in rat brain tissue *in vitro* and produces typical opioid-mediated effects *in vivo*. The analgesic potency of U-47700 is about 10-fold greater than that of morphine in the rat. Plasma concentrations of U-47700 and *N,N*-didesmethyl-U47700 rise linearly as dose increases, whereas *N*-desmethyl-U-47700 appears to accumulate in a nonlinear fashion. Pharmacodynamic effects of U-47700 are positively correlated with concentrations of U-47700 and its *N*-desmethylated metabolite, but both *N*-desmethyl metabolites display much weaker affinity for the μ-opioid receptor when compared to the parent compound. Correlation data examining U-47700 concentrations and hot plate latency demonstrate a counter clockwise hysteresis progression over time. Accumulating evidence shows that non-fentanyl NSOs, including various analogs of U-47700, are appearing in recreational drug markets worldwide (42). Information about the biological effects of these new compounds is needed to inform stakeholders who are involved with responding to the threat of NSOs (43). To this end, the present approach for examining pharmacodynamic and pharmacokinetic measures in the laboratory rat might be useful for rapidly profiling the biological activity of U-47700 analogs and other newly-emerging drugs of abuse.

Acknowledgements

This research was generously supported by the Intramural Research Program of the National Institute on Drug Abuse, National Institutes of Health (DA 00523 to MHB).

References

1. Jannetto PJ, Helander A, Garg U, Janis GC, Goldberger B, Ketha H. (2019) The Fentanyl Epidemic and Evolution of Fentanyl Analogs in the United States and the European Union. Clinical Chemistry, 65, 242–253. [PubMed: 30305277]
2. Prekupec MP, Mansky PA, Baumann MH. (2017) Misuse of Novel Synthetic Opioids: A Deadly New Trend. Journal of Addiction Medicine, 11, 256–265. [PubMed: 28590391]
3. Drug Enforcement Administration DoJ. (2016) Schedules of Controlled Substances: Temporary Placement of U-47700 Into Schedule I. Final order. Federal register, 81, 79389. [PubMed: 27905978]
4. Cheney BV, Szmuszkovicz J, Lahti RA, Zichi DA. (1985) Factors affecting binding of trans-N-[2-(methylamino)cyclohexyl]benzamides at the primary morphine receptor Journal of Medical Chemistry, 28, 1853–1864.
5. Baumann MH, Majumdar S, Le Rouzic V, Hunkele A, Uprety R, Huang XP, Xu J, Roth BL, Pan YX, Pasternak GW. (2018) Pharmacological characterization of novel synthetic opioids (NSO) found in the recreational drug marketplace. Neuropharmacology, 134, 101–107. [PubMed: 28807672]
6. Coopman V, Blanckaert P, Van Parys G, Van Calenbergh S, Cordonnier J. (2016) A case of acute intoxication due to combined use of fentanyl and 3,4-dichloro-N-[2-(dimethylamino)cyclohexyl]-N-methylbenzamide (U-47700). Forensic Science International, 266, 68–72. [PubMed: 27235591]
7. Rohrig TP, Miller SA, Baird TR. (2017) U-47700: A Not So New Opioid. Journal of Analytical Toxicology, 42, e12–e14.
8. Mohr ALA, Friscia M, Papsun D, Kacinko SL, Buzby D, Logan BK. (2016) Analysis of Novel Synthetic Opioids U-47700, U-50488 and Furanyl Fentanyl by LC-MS/MS in Postmortem Casework. Journal of Analytical Toxicology, 40, 709–717. [PubMed: 27590036]
9. Dziadosz M, Klintschar M, Teske J. (2017) Postmortem concentration distribution in fatal cases involving the synthetic opioid U-47700. International Journal of Legal Medicine, 131, 1555–1556. [PubMed: 28401304]
10. Elliott SP, Brandt SD, Smith C. (2016) The first reported fatality associated with the synthetic opioid 3,4-dichloro-N-[2-(dimethylamino)cyclohexyl]-N-methylbenzamide (U-47700) and implications for forensic analysis. Drug Testing and Analysis, 8, 875–879. [PubMed: 27232154]
11. Papsun D, Hawes A, Mohr ALA, Friscia M, Logan BK. (2017) Case Series of Novel Illicit Opioid-Related Deaths. Academic Forensic Pathology, 7, 477–486. [PubMed: 31239996]
12. Richeval C, Gaulier J-M, Romeuf L, Allorge D, Gaillard Y. (2019) Case report: relevance of metabolite identification to detect new synthetic opioid intoxications illustrated by U-47700. International Journal of Legal Medicine, 133, 133–142. [PubMed: 30443678]
13. Ellefsen KN, Taylor EA, Simmons P, Willoughby V, Hall BJ. (2017) Multiple Drug-Toxicity Involving Novel Psychoactive Substances, 3-Fluorophenmetrazine and U-47700. Journal of Analytical Toxicology, 41, 765–770. [PubMed: 28985320]
14. Partridge E, Trobbiani S, Stockham P, Charlwood C, Kostakis C. (2018) A Case Study Involving U-47700, Diclazepam and Flubromazepam—Application of Retrospective Analysis of HRMS Data. Journal of Analytical Toxicology, 42, 655–660. [PubMed: 29945197]
15. Gerace E, Salomone A, Luciano C, Di Corcia D, Vincenti M. (2018) First Case in Italy of Fatal Intoxication Involving the New Opioid U-47700. Frontiers in Pharmacology, 9.
16. Koch K, Auwärter V, Hermanns-Clausen M, Wilde M, Neukamm MA. (2018) Mixed intoxication by the synthetic opioid U-47700 and the benzodiazepine flubromazepam with lethal outcome: Pharmacokinetic data. Drug Testing and Analysis, 10, 1336–1341.

17. Strehmel N, Dümpelmann D, Vejmelka E, Strehmel V, Roscher S, Scholtis S, Tsokos M. (2018) Another fatal case related to the recreational abuse of U-47700. Forensic Science, Medicine and Pathology, 14, 531–535.
18. Garneau B, Desharnais B, Beauchamp-Doré A, Lavallée C, Mireault P, Lajeunesse A. (2019) Challenges Related to Three Cases of Fatal Intoxication to Multiple Novel Synthetic Opioids. Journal of Analytical Toxicology.
19. Fogarty MF, Papsun DM, Logan BK. (2018) Analysis of Fentanyl and 18 Novel Fentanyl Analogs and Metabolites by LC-MS-MS, and report of Fatalities Associated with Methoxyacetylfentanyl and Cyclopropylfentanyl. Journal of Analytical Toxicology, 42, 592–604. [PubMed: 29750250]
20. Vogliardi S, Stocchero G, Maietti S, Tucci M, Nalesso A, Snenghi R, Favretto D. (2018) Non-fatal Overdose with U-47700: Identification in Biological Matrices. Current Pharmaceutical Biotechnology, 19, 180–187. [PubMed: 29745328]
21. Židková M, Horsley R, Hloch O, Hložek T. (2019) Near-fatal Intoxication with the “New” Synthetic Opioid U-47700: The First Reported Case in the Czech Republic. Journal of Forensic Sciences, 64, 647–650. [PubMed: 30229896]
22. Krotulski AJ, Mohr ALA, Papsun DM, Logan BK. (2018) Metabolism of novel opioid agonists U-47700 and U-49900 using human liver microsomes with confirmation in authentic urine specimens from drug users. Drug Testing and Analysis, 10, 127–136. [PubMed: 28608586]
23. Jones MJ, Hernandez BS, Janis GC, Stellpflug SJ. (2017) A case of U-47700 overdose with laboratory confirmation and metabolite identification. Clinical Toxicology, 55, 55–59. [PubMed: 27549165]
24. Smith CR, Truver MT, Swortwood MJ. (2019) Quantification of U-47700 and its metabolites in plasma by LC-MS/MS. Journal of Chromatography B, 1112, 41–47.
25. Rojek S, Romańczuk A, Kula K, Synowiec K, Kłys M. (2019) Quantification of U-47700 and its metabolites: N-desmethyl-U-47700 and N,N-didesmethyl-U-47700 in 12 autopsy blood samples employing SPE/LC-ESI-MS-MS. Forensic Toxicology.
26. Carlier J, Wohlfarth A, Salmeron BD, Scheidweiler KB, Huestis MA, Baumann MH. (2018) Pharmacodynamic Effects, Pharmacokinetics, and Metabolism of the Synthetic Cannabinoid AM-2201 in Male Rats. Journal of Pharmacology and Experimental Theraputics, 367, 543–550.
27. Wong B, Perkins MW, Tressler J, Rodriguez A, Devorak J, Sciuto AM. (2017) Effects of inhaled aerosolized carfentanil on real-time physiological responses in mice: a preliminary evaluation of naloxone. Inhalation Toxicology, 29, 65–74. [PubMed: 28330429]
28. Truong PM, Hassan SA, Lee YS, Kopajtic TA, Katz JL, Chadderdon AM, Traynor JR, Deschamps JR, Jacobson AE, Rice KC. (2017) Modulation of opioid receptor affinity and efficacy via N-substitution of 9beta-hydroxy-5-(3-hydroxyphenyl)morphan: Synthesis and computer simulation study. Bioorganic and Medicinal Chemistry, 25, 2406–2422. [PubMed: 28314512]
29. Gunn A, Bobeck EN, Weber C, Morgan MM. (2011) The influence of non-nociceptive factors on hot-plate latency in rats. Journal of Pain, 12, 222–7. [PubMed: 20797920]
30. Taracha E, Mierzejewski P, Lehner M, Chrapusta SJ, Kala M, Lechowicz W, Hamed A, Skorzewska A, Kostowski W, Plaznik A. (2009) Stress-opioid interactions: a comparison of morphine and methadone. Pharmacological Reports, 61, 424–35. [PubMed: 19605941]
31. Van Ree JM, Leys A. (1985) Behavioral effects of morphine and phencyclidine in rats: the influence of repeated testing before and after single treatment. European Journal of Pharmacology, 113, 353–62. [PubMed: 2931287]
32. Poyhia R, Kalso EA. (1992) Antinociceptive effects and central nervous system depression caused by oxycodone and morphine in rats. Basic and Clinical Pharmacology and Toxicology, 70, 125–30.
33. Bergh MS, Bogen IL, Garibay N, Baumann MH. (2019) Evidence for nonlinear accumulation of the ultrapotent fentanyl analog, carfentanil, after systemic administration to male rats. Neuropharmacology, 158, 107596. [PubMed: 30965021]
34. Rawls SM, Benamar K. (2011) Effects of opioids, cannabinoids, and vanilloids on body temperature. Frontiers in Bioscience, 3, 822–45.
35. Iwamoto K, Klaassen CD. (1977) First-pass effect of morphine in rats. Journal of Pharmacology and Experimental Theraputics, 200, 236–44.

36. Miyamoto Y, Ozaki M, Yamamoto H. (1988) Effects of adrenalectomy on pharmacokinetics and antinociceptive activity of morphine in rats. Japanese Journal of Pharmacology, 46, 379–86. [PubMed: 3404768]

37. Armenian P, Olson A, Anaya A, Kurtz A, Ruegner R, Gerona RR. Fentanyl and a Novel Synthetic Opioid U-47700 Masquerading as Street “Norco” in Central California: A Case Report. Annals of Emergency Medicine.

38. Vo KT, van Wijk XMR, Wu AHB, Lynch KL, Ho RY. (2017) Synthetic agents off the darknet: a case of U-47700 and phenazepam abuse. Clinical Toxicology, 55, 71–72. [PubMed: 27736261]

39. Mahmood I (1998) Interspecies scaling: predicting volumes, mean residence time and elimination half-life. Some suggestions. Journals of Pharmacy and Pharmacology, 50, 493–499.

40. Theil FP, Guentert TW, Haddad S, Poulin P. (2003) Utility of physiologically based pharmacokinetic models to drug development and rational drug discovery candidate selection. Toxicology Letters, 138, 29–49. [PubMed: 12559691]

41. van Crugten JT, Somogyi AA, Nation RL, Reynolds G. (1997) Concentration-effect relationships of morphine and morphine-6β-glucuronide in the rat. Clinical and Experimental Pharmacology and Physiology, 24, 359–364. [PubMed: 9143788]

42. Sharma KK, Hales TG, Rao VJ, NicDaeid N, McKenzie C. (2019) The search for the “next” euphoric non-fentanil novel synthetic opioids on the illicit drugs market: current status and horizon scanning. Forensic Toxicol, 37, 1–16. [PubMed: 30636980]

43. Baumann MH, Kopajtic TA, Madras BK. (2018) Pharmacological Research as a Key Component in Mitigating the Opioid Overdose Crisis. Trends in Pharmacological Science, 39, 995–998.

- U-47700 induced dose-related increase in hot plate latency & catalepsy in male rats
- Pharmacodynamic effects were correlated with plasma U-47700 and its metabolite
- U-47700 displayed high affinity for μ receptor but metabolites were 10x weaker

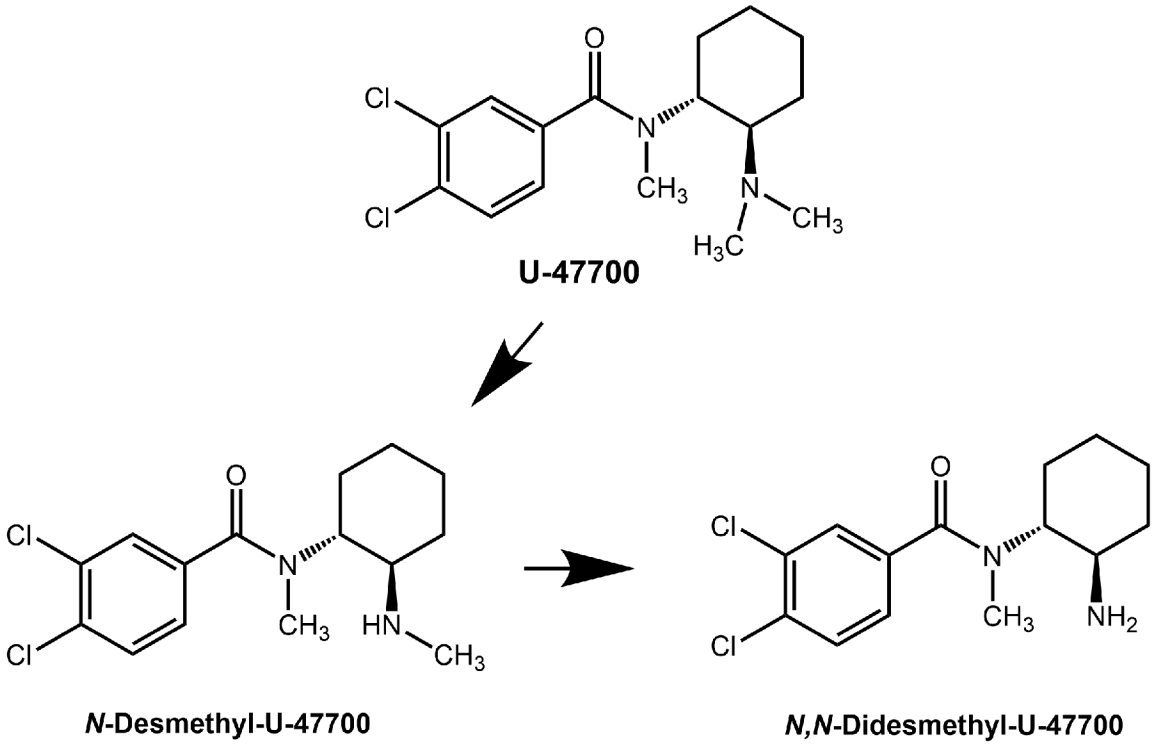

Figure 1.
Chemical structures of U-47700 and its main metabolites

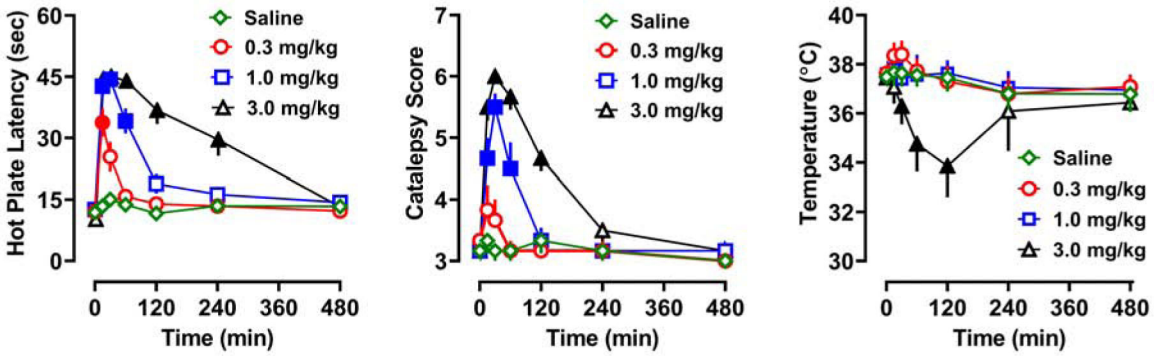

Figure 2.

Time-course of pharmacodynamic effects induced by s.c. saline or U-47700 (0.3, 1.0, and 3.0 mg/kg) in male rats. Hot plate latency, catalepsy score, and core body temperature are presented as mean±SEM for N=6 rats in saline, 0.3, and 1.0 mg/kg groups, and N=5 rats in the 3.0 mg/kg group. Filled symbols represent significant differences when compared to saline-treated group at a given time point ($p<0.05$, Tukey's).

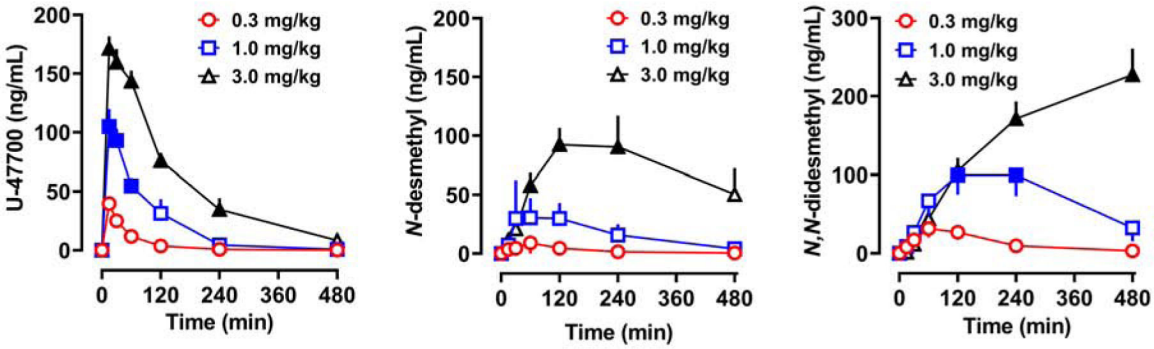

Figure 3.

Time-concentration profiles for U-47700, *N*-desmethyl-U-47700 (*N*-desmethyl), and *N,N*-didesmethyl-U-47700 (*N,N*-didesmethyl) after s.c. injection of U-47700. Findings presented in Figure 3 are from the same rats depicted in Figure 2. Data are mean±SEM for N=6 rats in the 0.3 and 1.0 mg/kg groups, and N=5 rats in the 3.0 mg/kg group. Filled symbols represent significant differences when compared to the low dose (0.3 mg/kg) group at a given time point ($p<0.05$, Tukey's).

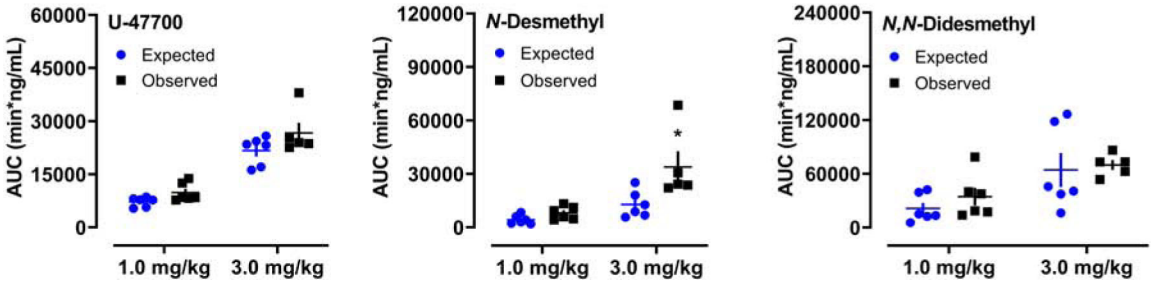

Figure 4.

Comparison of expected versus observed AUC values for U-47700, *N*-desmethyl-U-47700 (*N*-desmethyl), and *N,N*-didesmethyl-U-47700 (*N,N*-didesmethyl) after s.c. administration of U-47700. Expected values for the 1.0 and 3.0 doses were calculated by multiplying the observed AUC values at 0.3 mg/kg U-47700 by a factor of 3.3 and 10, respectively. Data are mean±SEM. * = significant difference from corresponding expected value ($p<0.05$).

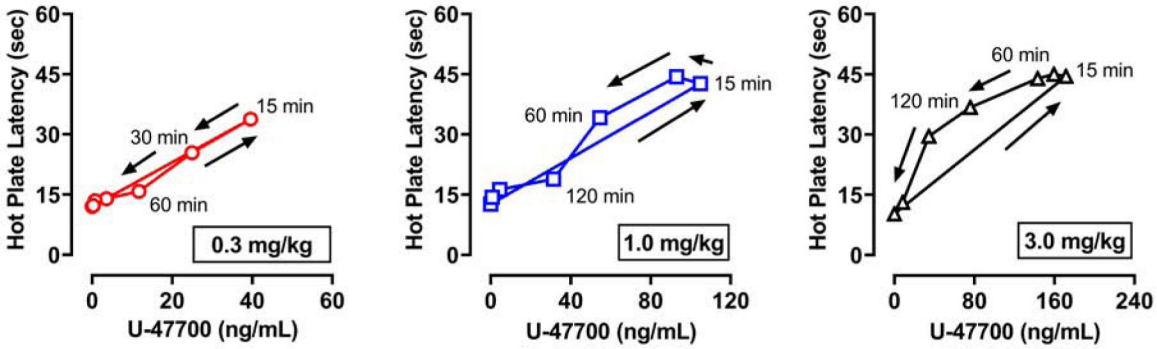

Figure 5.

Hysteresis plots for mean hot plate latency values versus U-47700 plasma concentrations at each dose of drug administered. Data are mean±SEM for N=6 rats in the 0.3 and 1.0 mg/kg groups, and N=5 rats in the 3.0 mg/kg group. Arrows represent hysteresis curve progression over time for 480 min.

Table 1.

Pharmacokinetic constants for U-47700 and its *N*-desmethyl metabolites after s.c. administration of 0.3, 1.0, or 3.0 mg/kg U-47700 in male rats.

Analyte	Dose (mg/kg)	C_{max} (ng/mL)	T_{max} (min)	AUC (min*ng/mL)	$t_{1/2}$ (min)	C_{last} (ng/mL)
U-47700	0.3	40±3	15	2169±164	82±9	0.2±0.1
	1.0	110±13	38±17	9872±1063	68±4	0.8±0.3
	3.0	173±9	24±9	26692±2861	102±16	8±4
***N*-Desmethyl-U-47700**	0.3	9±4	80±13	1289±306	110±7	0.4±0.1
	1.0	46±11	75±15	8158±1526	136±17	4±1
	3.0	102±23	168±29	33881±8794	-	76±31
***N*,*N*-Didesmethyl-U-47700**	0.3	32±11	90±13	6427±1890	126±10	3±1
	1.0	108±26	160±25	34463±9920	301±84	32±17
	3.0	236±31	384±59	69834±5492	-	191±46

Data are expressed as mean±SEM for N=5–6 rats/group.

Table 2.

Opioid receptor binding affinities for U-47700 and its *N*-desmethyl metabolites in post-mortem rat brain tissue.

Compound	μ-opioid receptor Ki (nM)	δ-opioid receptor Ki (nM)	κ-opioid receptor Ki (nM)	μ/δ ratio	μ/κ ratio
U-47700	11.1±0.4	1220±82	287±24	110	26
***N*-Desmethyl-U-47700**	206±11	>10,000	1730±196	>49	8
***N,N*-Didesmethyl-U-47700**	4080±304	>10000	6770±814	>2	>2
Morphine	2.7±0.3	261±24	101±9	97	37

Data are expressed as mean±SEM for N=3 experiments performed in triplicate.